Hindawi
International Journal of Antennas and Propagation
Volume 2017, Article ID 5719835, 13 pages
https://doi.org/10.1155/2017/5719835

Research Article

A Frequency-Tracking and Impedance-Matching Combined System for Robust Wireless Power Transfer

Yanting Luo, Yongmin Yang, Suiyu Chen, and Xisen Wen

Science and Technology on Integrated Logistics Support Laboratory, National University of Defense Technology, Changsha 410073, China

Correspondence should be addressed to Yongmin Yang; yangyongmin@163.com

Received 23 September 2016; Revised 12 December 2016; Accepted 4 January 2017; Published 29 January 2017

Academic Editor: Luciano Tarricone

One of the greatest challenges to power embedded devices using magnetically coupled resonant wireless power transfer (WPT) system is that the amount of power delivered to the load is very sensitive to load impedance variations. Previous adaptive impedance-matching (IM) technologies have drawbacks because adding IM networks, relay coils, or other compensating components in the receiver-side will significantly increase the receiver size. In this paper, a novel frequency-tracking and impedance-matching combined system is proposed to improve the robustness of wireless power transfer for embedded devices. The characteristics of the improved WPT system are investigated theoretically based on the two-port network model. Simulation and experimental studies are carried out to validate the proposed system. The results suggest that the frequency-tracking and impedance-matching combined WPT system can quickly find the best matching points and maintain high power transmission efficiency and output power when the load impedance changes.

1. Introduction

Magnetically coupled resonant wireless power transfer (WPT) is one of the most potential technologies to solve the energy problems for embedded devices. The built-in battery is not a desired power source because it always limits system size and its replacement needs disassembling the device for most embedded applications [1–4]. By making use of WPT technology, embedded devices can be powered effectively without changing batteries or increasing battery size, which contribute to realizing a compact-sized, long-life embedded system.

One of the greatest challenges to power embedded devices using WPT technology is that the amount of power delivered to the load is very sensitive to load impedance variations [5–9]. For example, when an ultracapacitor is being charged, the load can be seen as an increasing instantaneous impedance. However, the ultracapacitor only receives the maximum power at a single optimal impedance [6]. At other impedances, the power delivered to the ultracapacitor decreases rapidly due to impedance mismatch. Moreover, in some applications, there is a need to power multiple embedded devices using one power transmitter [7–9]. Therefore, the total load impedance depends on how many devices are being powered simultaneously. But the output power of the WPT system only reaches the maximum value at an optimal load impedance as well. For these reasons, it is important to develop adaptive impedance-matching (IM) technology to quickly find the best impedance points [10].

Many works have been done on the adaptive impedance-matching technology for the WPT system, including the following: (1) adjusting the source operating frequency until the output power of the WPT system is maximized [11–14], (2) adding variable impedance-matching networks in the WPT system to transform the input and output impedance to optimal values [15–18], (3) optimizing the mutual inductance between coils using multicoil topology [19–23], and (4) using a receiver-side switching converter to transform the actual load resistance into optimal load resistance [5, 24–26].

For many WPT systems, the operating frequency is fixed or limited to a very narrow band. Meanwhile, in some cases, because the operating frequency may not be optimal

depending on factors such as load variations, the frequency-tuning approach has been adopted and shown its advantages [11–14]. In [13], the source operating frequency is adjusted to compensate for changes in the input impedance of the WPT system until the imaginary part of the input impedance becomes zero. Their experimental results show that the output power of the WPT system can be improved by optimizing the operating frequency. This method is simple to implement but cannot work well in weakly coupled WPT systems.

In [18], two variable IM networks are inserted in the transmitter circuit and the receiver circuit, respectively. By doing so, both the transmitter circuit and the receiver circuit can be adjusted to satisfy conjugate impedance-matching conditions through feedback control. Although this approach can achieve higher output power than frequency-tuning, it needs additional IM networks and control components in both the transmitter circuit and the receiver circuit, which will inevitably increase the system size.

In [20], a WPT system topology which includes an excitation-coil, a transmitter coil, a receiver coil, and a pickup-coil is proposed for automatic impedance-matching purpose. An actuator is used to change the relative position of coils to match the impedance of the WPT system. However, using four-coil topology will also increase the system complexity and energy consumption.

In [24], a novel GaN Buck converter is used to emulate a variable load resistor to adjust the WPT system for maximum efficiency or received power, thereby eliminating the requirements of using IM networks. In [5], a switching converter is added in the receiver-side to automatically transform the load resistance into a desired value. Experimental results demonstrate that the WPT system can obtain high efficiency under load resistance variations.

In order to ensure a compact embedded system, the receiver should be designed as small as possible [27–29]. Thus, previous adaptive impedance-matching approaches have drawbacks because adding IM networks, relay coils, or switching converters with their control circuits in the receiver-side will significantly increase the system size. In this paper, a novel frequency-tracking and impedance-matching combined system is proposed to improve the robustness of wireless power transfer for embedded devices. To quickly find the best matching points, the source operating frequency is automatically optimized at first, and then a variable IM network in the transmitter circuit is used to match the system's input impedance to the source impedance. Through this approach, both the power transmission efficiency and the output power of the WPT system can be significantly improved. The proposed system is validated through numerical simulations and experimental measurements.

The rest of the paper is organized as follows. Section 2 describes the traditional dual-side conjugated IM principle for the WPT system. Section 3 presents the frequency-tracking and impedance-matching combined system. The characteristics of the improved WPT system are analyzed based on the two-port network theory and the effects of load impedance change on the power transmission efficiency and output power are investigated through numerical simulations. Experimental measurements are evaluated in Section 4. As a comparison, the calculated and measured results of the original WPT system, the dual-side impedance-matching WPT system, and the frequency-tracking and impedance-matching combined WPT system are provided as well. Finally, conclusions are drawn in Section 5.

2. Traditional Dual-Side IM Principle

Figure 1 shows the circuit model of a series-compensated WPT system, which consists of a power source, a coupled resonators-circuit, and a load. U_S, ω, and Z_S are the voltage, angular frequency, and internal impedance of the power source, respectively. L_T and L_R are the inductances of the transmitter coil and the receiver coil, respectively. R_T and R_R are the equivalent resistances of the transmitter coil and the receiver coil, respectively. M is the mutual inductance between coils. In order to achieve resonance, two lumped capacitors, C_T and C_R, are connected to the transmitter coil and the receiver coil, respectively. Z_{in} and Z_{out} are the input impedance and output impedance of the resonators-circuit, respectively. Z_L is the load impedance.

To simplify the analysis, the circuit model shown in Figure 1 is seen as a two-port network. According to the maximum power transfer theorem [14, 30], if the two-port network satisfies the dual-side conjugate impedance-matching equation

$$\begin{aligned} Z_{\text{in}} &= Z_S^*, \\ Z_{\text{out}} &= Z_L^* \end{aligned} \tag{1}$$

the power delivered to the load will be maximized, where Z_S^* is the conjugate value of Z_S and Z_L^* is the conjugate value of Z_L.

For a constant load impedance Z_L, (1) can be easily satisfied by optimizing the parameters of the WPT system. However, if Z_L changes, the dual-side conjugate impedance-matching equation can only be satisfied at an optimal load impedance. At other load impedances, the output power of the WPT system will decrease rapidly due to impedance mismatching.

In a practical WPT system, the load impedance may change due to many factors, like load temperature rise, operating mode switching, and so on [5–9]. The output power of the WPT system will become unstable if the load impedance changes and this will cause serious problems in most engineering applications. In order to maintain the maximum output power, the dual-side impedance-matching system is proposed in [14, 18]. In their systems, two controllable IM networks are added in the transmitter circuit and the receiver circuit, respectively, as shown in Figure 2. Thus, the input and output impedance of the WPT system can be automatically adjusted to satisfy (1) through scattering-parameters or reflected coefficient feedback control. Then, the output power of the WPT system can maintain the maximum value when the load impedance changes.

However, the dual-side IM approach has some drawbacks, especially when it is used in the WPT system for embedded applications. Since spaces in most embedded

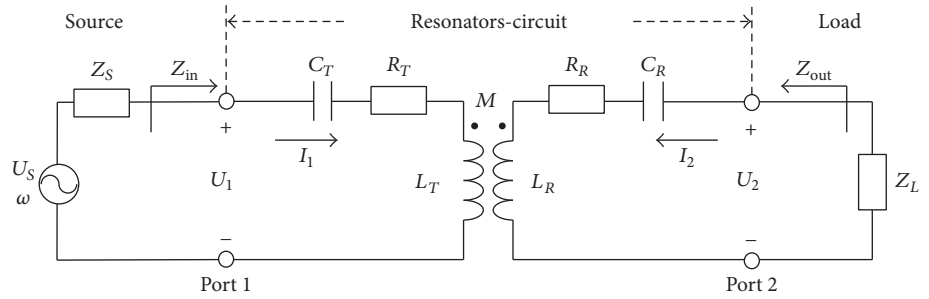

Figure 1: Circuit model of a series-compensated WPT system.

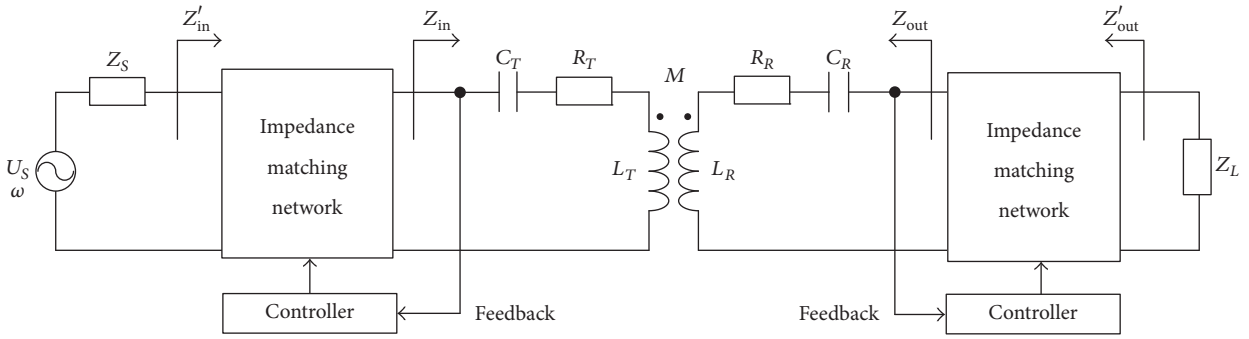

Figure 2: Traditional dual-side impedance-matching system.

devices are not available to accommodate too many circuits and components, the size of the power receiver should be as small as possible [27–29]. The dual-side IM approach needs additional variable IM networks and control components in the receiver circuit, which will obviously increase the receiver size and weight. Moreover, more IM components in the receiver means more energy consumption and less power delivered to the load. To overcome these drawbacks, a frequency-tracking and impedance-matching combined system is proposed in the next section.

3. The Proposed Frequency-Tracking and Impedance-Matching Combined WPT System

3.1. Modeling and Optimization. The proposed frequency-tracking and impedance-matching combined WPT system is shown in Figure 3. It includes a frequency-adjustable power source, an IM network in the transmitter circuit, which contains two variable components, a coupled resonators-circuit, and a load. In the WPT system, the variable IM network is used to match the transmitter's impedance to the source impedance through feedback control. The source operating frequency is adjusted to change the receiver's impedance instead of using another variable IM network, which can simplify the structure of the receiver circuit.

The circuit model shown in Figure 3 can be looked at as a cascade connection of the power source, the variable IM network, the coupled resonators-circuit, and the load. For simplicity, the characteristics of them are analyzed separately.

3.1.1. Coupled Resonators-Circuit. Based on the two-port network theory [31–33], the transmission matrix equation can be used to describe the input and output characteristics of the resonators-circuit, as

$$\begin{bmatrix} U_1 \\ I_1 \end{bmatrix} = \begin{bmatrix} A & B \\ C & D \end{bmatrix} \begin{bmatrix} U_2 \\ I_2 \end{bmatrix}, \tag{2}$$

where U_1 and I_1 are the input voltage and current at port 1, respectively. U_2 and I_2 are the input voltage and current at port 2, respectively. A, B, C, and D are the transmission parameters of the coupled resonators-circuit. For a series-compensated wireless power transfer system, A, B, C, and D can be calculated as follows: $A = (R_T + j\omega L_T - j/\omega C_T)/j\omega M$, $B = [(R_R + j\omega L_R - j/\omega C_R)(R_T + j\omega L_T - j/\omega C_T) + \omega^2 M^2]/j\omega M$, $C = 1/j\omega M$, and $D = (R_R + j\omega L_R - j/\omega C_R)/j\omega M$.

From the circuit model shown in Figure 3, the input impedance at port 1 can be found:

$$Z_{in} = \frac{U_1}{I_1} = \frac{AZ_L + B}{CZ_L + D} = R_{in} + jX_{in}, \tag{3}$$

where R_{in} and X_{in} represent the real part and the imaginary part of Z_{in}, respectively. Substituting A, B, C, and D parameters into (3) yields

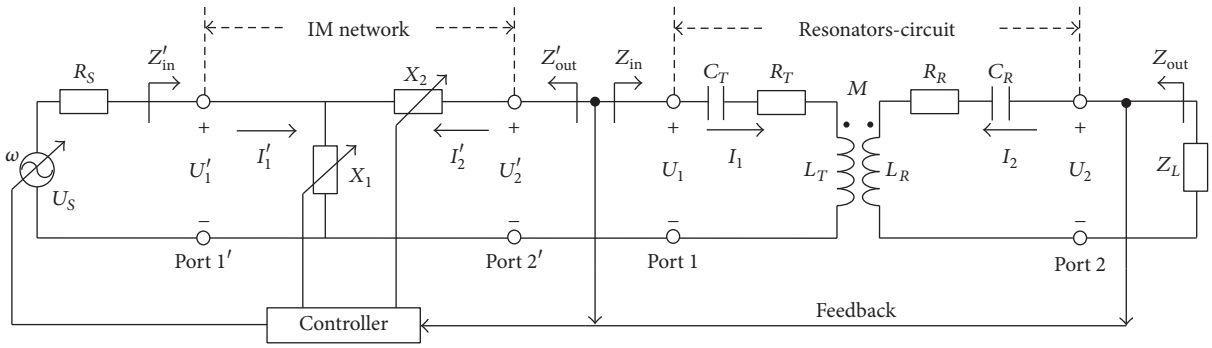

Figure 3: Proposed frequency-tracking and impedance-matching combined WPT system.

$$R_{\text{in}} = \frac{R_T\left(R_R + R_L\right)^2 + R_T\left(X_L + \omega L_R - 1/\omega C_R\right)^2 + R_R\omega^2M^2 + R_L\omega^2M^2}{\left(R_R + R_L\right)^2 + \left(X_L + \omega L_R - 1/\omega C_R\right)^2},$$
$$X_{\text{in}} = \frac{\left(\omega L_T - 1/\omega C_T\right)\left[\left(R_R + R_L\right)^2 + \left(X_L + \omega L_R - 1/\omega C_R\right)^2\right] - \omega^2M^2\left(X_L + \omega L_R - 1/\omega C_R\right)}{\left(R_R + R_L\right)^2 + \left(X_L + \omega L_R - 1/\omega C_R\right)^2}. \tag{4}$$

Then, the input active power at port 1 can be calculated by

$$P_{\text{in}} = \left|I_1^2\right| R_{\text{in}}. \tag{5}$$

Because the load in a practical system may not be a pure resistance [34, 35], the load impedance Z_L is assumed to be $R_L + jX_L$, where R_L and X_L represent the resistance and reactance of the load, respectively. Then, the output active power at port 2 can be calculated by

$$P_{\text{out}} = \left|I_2^2\right| R_L. \tag{6}$$

In previous studies, two kinds of power transfer efficiencies are defined to analyze the performance of the WPT system [36–38]. The system efficiency η_S refers to the ratio of the output power P_{out} at port 2 and total input power P_S from the wall outlet. It considers both the power losses in the AC power source and the resonators-circuit. Therefore, the system efficiency η_S cannot exceed 50% if the conjugate impedance-matching theorem is adopted because the source internal resistance will consume a half of the total input power P_S. The power transmission efficiency η_T is the ratio of the output power P_{out} at port 2 and the input power at port 1 P_{in}. It only includes the power losses in the resonators-circuit. In this paper, because the goal is not to improve the system power efficiency, the power transmission efficiency η_T is used to characterize the WPT system. η_T can be calculated using

$$\eta_T = \frac{P_{\text{out}}}{P_{\text{in}}}. \tag{7}$$

By substituting (5) and (6) into (7), the power transmission efficiency of the resonators-circuit can be found:

$$\eta_T = \frac{\omega^2M^2R_L}{R_T\left(R_R + R_L\right)^2 + \left(R_R + R_L\right)\omega^2M^2 + R_T\left(X_L + \omega L_R - 1/\omega C_R\right)^2}. \tag{8}$$

3.1.2. IM Network. As shown in Figure 3, the IM network includes two compensating components. X_1 and X_2 are the values of them. The transmission matrix equation of the IM network can be expressed as

$$\begin{bmatrix} U'_1 \\ I'_1 \end{bmatrix} = \begin{bmatrix} A' & B' \\ C' & D' \end{bmatrix} \begin{bmatrix} U'_2 \\ I'_2 \end{bmatrix}, \tag{9}$$

where U'_1 and I'_1 are the input voltage and current at port 1′, respectively. U'_2 and I'_2 are the input voltage and current at port 2′, respectively. A', B', C', and D' are the transmission parameters of the IM network. Based on the structure of the IM network, A', B', C', and D' can be calculated as follows: $A' = 1$, $B' = jX_2$, $C' = 1/jX_1$, and $D' = (X_1 + X_2)/X_1$.

Then, the input impedance at port 1′ can be found:

$$Z'_{\text{in}} = \frac{U'_1}{I'_1} = \frac{A'Z_{\text{in}} + B'}{C'Z_{\text{in}} + D'} = R'_{\text{in}} + jX'_{\text{in}}, \tag{10}$$

where R'_{in} and X'_{in} represent the real part and the imaginary part of Z'_{in}, respectively. Substituting A', B', C', and D' parameters into (10) yields

$$R'_{\text{in}} = \frac{-X_1X_2R_{\text{in}} - X_1X_{\text{in}}R_{\text{in}} + \left(X_1 + X_2 + X_{\text{in}}\right)X_1R_{\text{in}}}{R_{\text{in}}^2 + \left(X_1 + X_2 + X_{\text{in}}\right)^2},$$
$$X'_{\text{in}} = \frac{X_1R_{\text{in}}^2 + \left(X_1 + X_2 + X_{\text{in}}\right)X_1X_2 + \left(X_1 + X_2 + X_{\text{in}}\right)X_1X_{\text{in}}}{R_{\text{in}}^2 + \left(X_1 + X_2 + X_{\text{in}}\right)^2}. \tag{11}$$

In this paper, the ratio of the output active power P'_{out} at port 2′ and input active power P'_{in} at port 1′ is defined as the

power transmission efficiency of the IM network. It can be calculated by

$$\eta_{\mathrm{IM}} = \frac{P'_{\mathrm{out}}}{P'_{\mathrm{in}}}, \tag{12}$$

where $P'_{\mathrm{in}} = |I'^2_1|R'_{\mathrm{in}}$ and $P'_{\mathrm{out}} = |I'^2_2|R_{\mathrm{in}}$.

Substituting (11) into (12) yields $\eta_{\mathrm{IM}} = 100\%$. This is because the compensating components are assumed to be ideal energy-storage components without any energy losses. But, in fact, X_1 and X_2 also consume part of the total energy in the forms of heat and radiation [39, 40]. Therefore, the power transmission efficiency of the IM network cannot reach 100% in a practical system. To simplify the analysis, η_{IM} is assumed to be 100% in the theoretical analysis.

3.1.3. Overall WPT System. By substituting $U'_2 = U_1$ and $I'_2 = -I_1$ into (2), the transmission matrix equation of the overall WPT system can be found:

$$\begin{bmatrix} U'_1 \\ I'_1 \end{bmatrix} = \begin{bmatrix} A' & B' \\ C' & D' \end{bmatrix} \begin{bmatrix} A & B \\ C & D \end{bmatrix} \begin{bmatrix} U_2 \\ I_2 \end{bmatrix}. \tag{13}$$

Thus, the power transmission efficiency of the overall WPT system can be calculated as

$$\eta_{\mathrm{total}} = \frac{P_{\mathrm{out}}}{P'_{\mathrm{in}}} = \frac{P'_{\mathrm{out}}}{P'_{\mathrm{in}}} \times \frac{P_{\mathrm{out}}}{P_{\mathrm{in}}} = \eta_{\mathrm{IM}}\eta_T. \tag{14}$$

Substituting (7) and (12) into (14) yields

$$\eta_{\mathrm{total}} = \frac{\omega^2 M^2 R_L \eta_{\mathrm{IM}}}{R_T\left(R_R + R_L\right)^2 + \left(R_R + R_L\right)\omega^2 M^2 + R_T\left(X_L + \omega L_R - 1/\omega C_R\right)^2}. \tag{15}$$

Then, the output active power P_{out} of the overall WPT system can be expressed as

$$P_{\mathrm{out}} = P'_{\mathrm{in}} \times \eta_{\mathrm{total}}. \tag{16}$$

From here it can be seen that the output power P_{out} is the function of the input power P'_{in} and the power transmission efficiency η_{total}. To maximize the output power of the WPT system, both P'_{in} and η_{total} should be improved.

3.1.4. Efficiency and Output Power Optimization. According to (15), the operating frequency can be adjusted to increase the power transmission efficiency η_{total}. By solving "$d\eta_{\mathrm{total}}/df = 0$," the optimal frequencies to maximize η_{total} can be found:

$$f_{\mathrm{opt}} = \begin{cases} \dfrac{\left(C_R + C_L\right)}{\pi\sqrt{4L_R C_R C_L^2 + 4L_R C_R^2 C_L - 2C_R^2 C_L^2\left(R_R + R_L\right)^2}}, & \text{for Capacitive Load,} \\ \dfrac{1}{\pi\sqrt{4L_R C_R + 4L_L C_R - 2C_R^2\left(R_R + R_L\right)^2}}, & \text{for Inductive Load,} \end{cases} \tag{17}$$

where $C_L = -1/\omega X_L$ represents the equivalent capacitance of a capacitive load and $L_L = X_L/\omega$ represents the equivalent inductance of inductive load. The operating frequency is $f = \omega/2\pi$.

To maximize the input active power P'_{in}, the IM network is used to conjugately match the input impedance Z'_{in} to the source impedance Z_S. Then the output power of the overall WPT system can be maximized because $P_{\mathrm{out}} = P'_{\mathrm{in}} \times \eta_{\mathrm{total}}$. By introducing (10) into $Z'_{\mathrm{in}} = Z_S^*$, the optimal values of X_1 and X_2 can be obtained:

$$\begin{aligned} X_{\mathrm{opt},1} &= \pm\frac{R_S R_{\mathrm{in}}}{\sqrt{R_S R_{\mathrm{in}} - R_{\mathrm{in}}^2}}, \\ X_{\mathrm{opt},2} &= -X_{\mathrm{in}} \pm \sqrt{R_S R_{\mathrm{in}} - R_{\mathrm{in}}^2}. \end{aligned} \tag{18}$$

The compensating components X_1 and X_2 can be realized using variable capacitors/inductances. The optimal values of the capacitors/inductances can be calculated by

$$\begin{aligned} L_{\mathrm{opt},i} &= \frac{X_{\mathrm{opt},i}}{2\pi f_{\mathrm{opt}}} \quad \text{if } X_{\mathrm{opt},i} > 0, \\ C_{\mathrm{opt},i} &= -\frac{1}{2\pi f_{\mathrm{opt}} X_{\mathrm{opt},i}} \quad \text{if } X_{\mathrm{opt},i} < 0, \\ & \qquad i = 1, 2. \end{aligned} \tag{19}$$

According to the analysis, when the load impedance changes, the power transmission efficiency and the output power of the WPT system can be optimized following these steps: (1) adjusting the source operating frequency f to the optimal frequency f_{opt} at first and (2) adjusting the variable components, X_1 and X_2, to the best matching point ($X_{\mathrm{opt},1}$, $X_{\mathrm{opt},2}$).

Table 1: Parameters used for calculations.

Parameters	Values
Source resistance R_S	50 Ω
Lumped capacitors C_T, C_R	216 pF
Coil resistance R_T, R_R	2 Ω
Coil inductance L_T, L_R	29 uH
Coil frequency f_T, f_R	2 MHz
Coupling coefficient k	0.13
Load resistance R_L	10~500 Ω
Load reactance X_L	−500~500 Ω

3.2. Numerical Simulations. In this section, the impacts of load impedance change on the power transmission efficiency η_{total} and output power P_{out} are investigated through numerical simulations. Two different situations, the load reactance change and the load resistance change, are considered separately. The parameters used for calculations are given in Table 1.

3.2.1. Power Transmission Efficiency. When the load reactance X_L increases from −500 Ω to 500 Ω, the power transmission efficiency of the WPT system can be obtained using (15). Figure 4(a) shows the calculated results of power transmission efficiency η_{total} versus load reactance X_L and source operating frequency f. When f is fixed at 2 MHz, it can be seen from Figure 4(a) that η_{total} increases firstly and then decreases with the increase of X_L, and the maximum power transmission efficiency can only be achieved at a single load reactance $X_L = 0\,\Omega$.

Figure 4(b) shows the calculated results of η_{total} versus load resistance R_L and source operating frequency f, where the load resistance R_L increases from 10 Ω to 500 Ω. From Figure 4(b), the similar trend can be found: when f is fixed at 2 MHz, η_{total} increases firstly and then decreases with the increase of R_L, and the maximum power transmission efficiency can only be achieved at an optimal load resistance $R_L = 50\,\Omega$.

Based on the theoretical analysis, the source operating frequency is adjusted to improve the power transmission efficiency firstly when the load impedance changes. The optimal frequencies f_{opt} for maximizing η_{total} can be calculated using (17). They are marked with blue dashed line in Figure 4. It can be observed that the WPT system can maintain high efficiency when the source frequency is adjusted along the optimal frequency line.

3.2.2. Output Power. Setting $X_L = -500, -250, 250, 500\,\Omega$ and $R_L = 100, 200, 300, 400\,\Omega$, respectively, yields corresponding optimal frequencies $f_{\text{opt}} \approx 3.11$, 2.64, 1.57, and 1.32 MHz and $f_{\text{opt}} \approx 2.05$, 2.18, 2.47, and 3.19 MHz. To increase the output power of the WPT system, the variable components X_1 and X_2 are used to match the impedance of the WPT system at the optimal frequencies.

Figures 5 and 6 show the calculated results of output power P_{out} versus X_1 and X_2. The best matching points $(X_{\text{opt},1}, X_{\text{opt},2})$ for maximizing P_{out} can be found using (18). They are marked with black points in Figures 5 and 6. It can be seen that P_{out} will reach the maximum value if X_1 and X_2 are adjusted to the best matching points.

From Figures 5 and 6, it can be seen that the numerical simulation results agree with the theoretical analysis well. The results suggest that the power transmission efficiency of the WPT system can be significantly improved by changing the source operating frequency f to the optimal frequency f_{opt}, and the output power can achieve high value by adjusting the IM network to the best matching point $(X_{\text{opt},1}, X_{\text{opt},2})$.

4. Experiments and Discussion

4.1. Hardware Implementation. To demonstrate the validity of the proposed frequency-tracking and impedance-matching combined approach for the WPT system, an experimental system is designed and implemented. Two circular air-core coils, which are fabricated by Litz wires, are used as the power transmitter and receiver. The radii of the transmitter coil and the receiver coil are 13 cm and 11 cm, and the number of turns of the two coils is 8. In order to compensate the reactive power, two lumped capacitors are connected to the transmitter coil and receiver coil, respectively. A signal generator, which has an adjustable frequency range of 1–10 MHz, is used to change the operating frequency of the power amplifier. An L-section impedance-matching network consisting of variable-capacitor and fixed-inductance arrays (as shown in Figure 7) is inserted in the transmitter circuit to match the input impedance Z'_{in} to the source impedance Z_S. Each variable air capacitor has a tunable range of 360 pF to 20 pF, for the rotation angle of $\theta = 0^\circ$ to $\theta = 180^\circ$, respectively. Small steering engines are used to change the rotation angle of the variable air capacitors through feedback control.

A directional power meter, which is connected between the power amplifier and the IM network, is used to measure the input power P'_{in}. A load, which includes a resistance R_L and a reactance X_L, is connected to the output port of the receiver coil. Another power meter is connected between the receiver coil and the load, providing output power P_{out} feedback to the transmitter-side through wireless communication. A controller is used to analyze the power transmission efficiency and the output power of the overall WPT system and change the output frequency of the signal generator and the rotation angle of the steering engines. The actual experimental system and the adaptive IM circuit are shown in Figures 8 and 9, respectively. An Agilent 4294A impedance analyzer is used to measure the precise electrical parameters of the experimental system, which are listed in Table 2.

When the load impedance changes, the WPT system can be automatically adjusted following these steps: (1) first step is adjusting the source operating frequency f until the measured power transmission efficiency η_{total} is maximized. The source operating frequency to achieve the maximum η_{total} is marked as the optimal frequency f_{opt}; (2) second step is adjusting the variable capacitors in the IM network at the optimal frequency until the measured output active power P'_{out} is maximized.

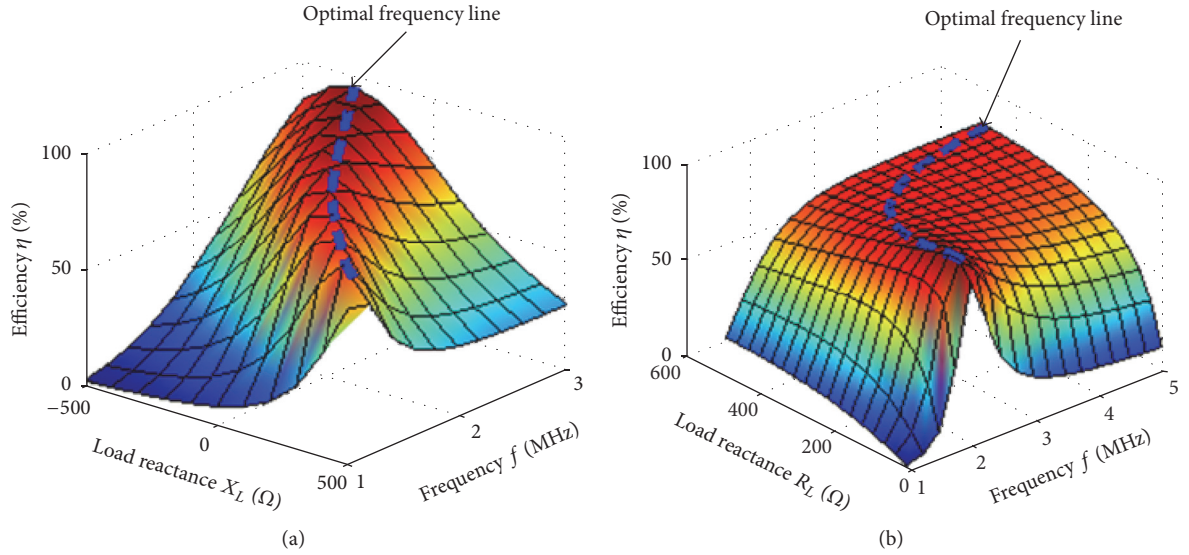

FIGURE 4: (a) Calculated η_{total} versus X_L and f. (b) Calculated η_{total} versus R_L and f.

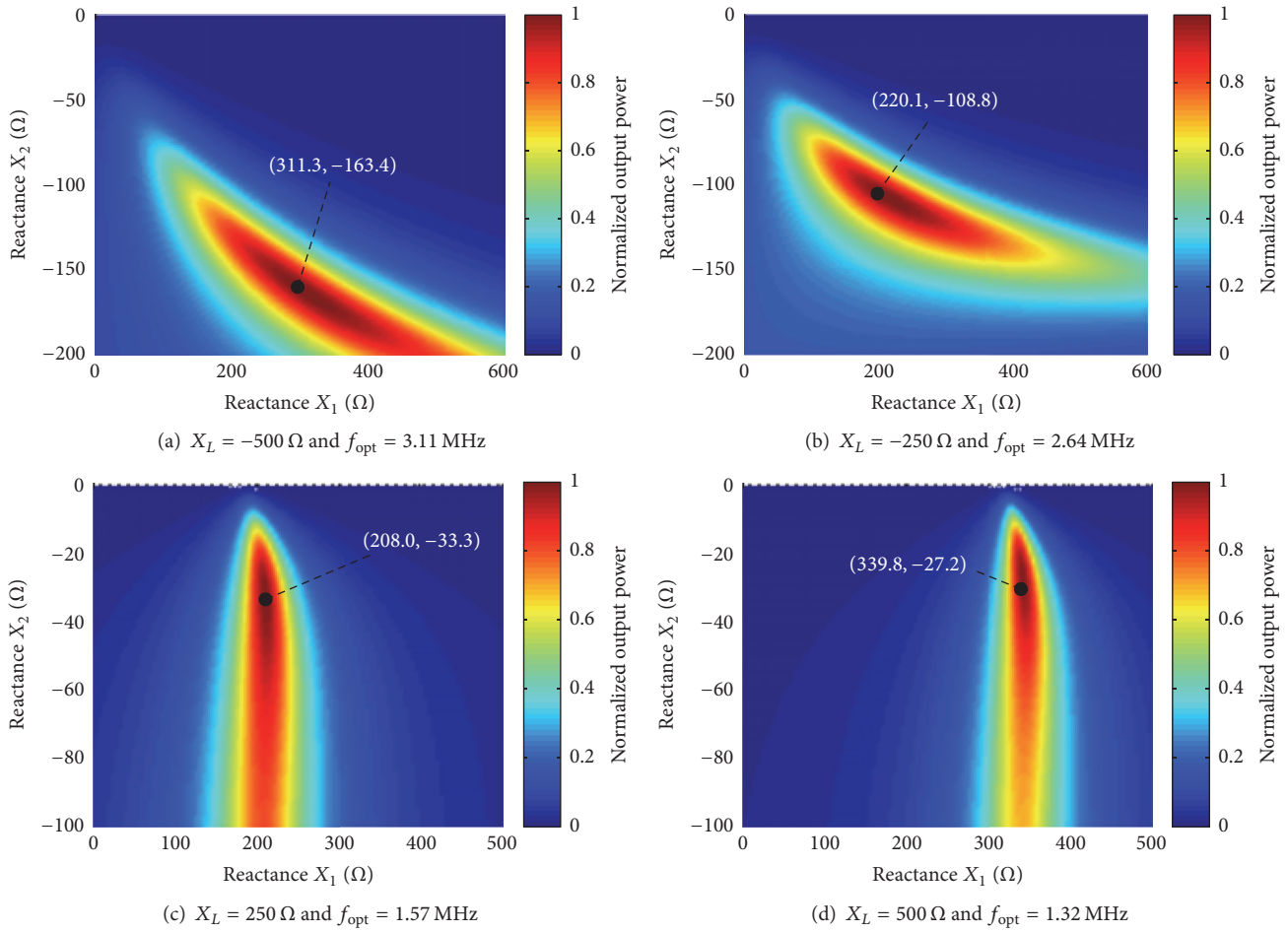

FIGURE 5: Calculated P_{out} versus X_1 and X_2. The load resistance $R_L = 100\,\Omega$.

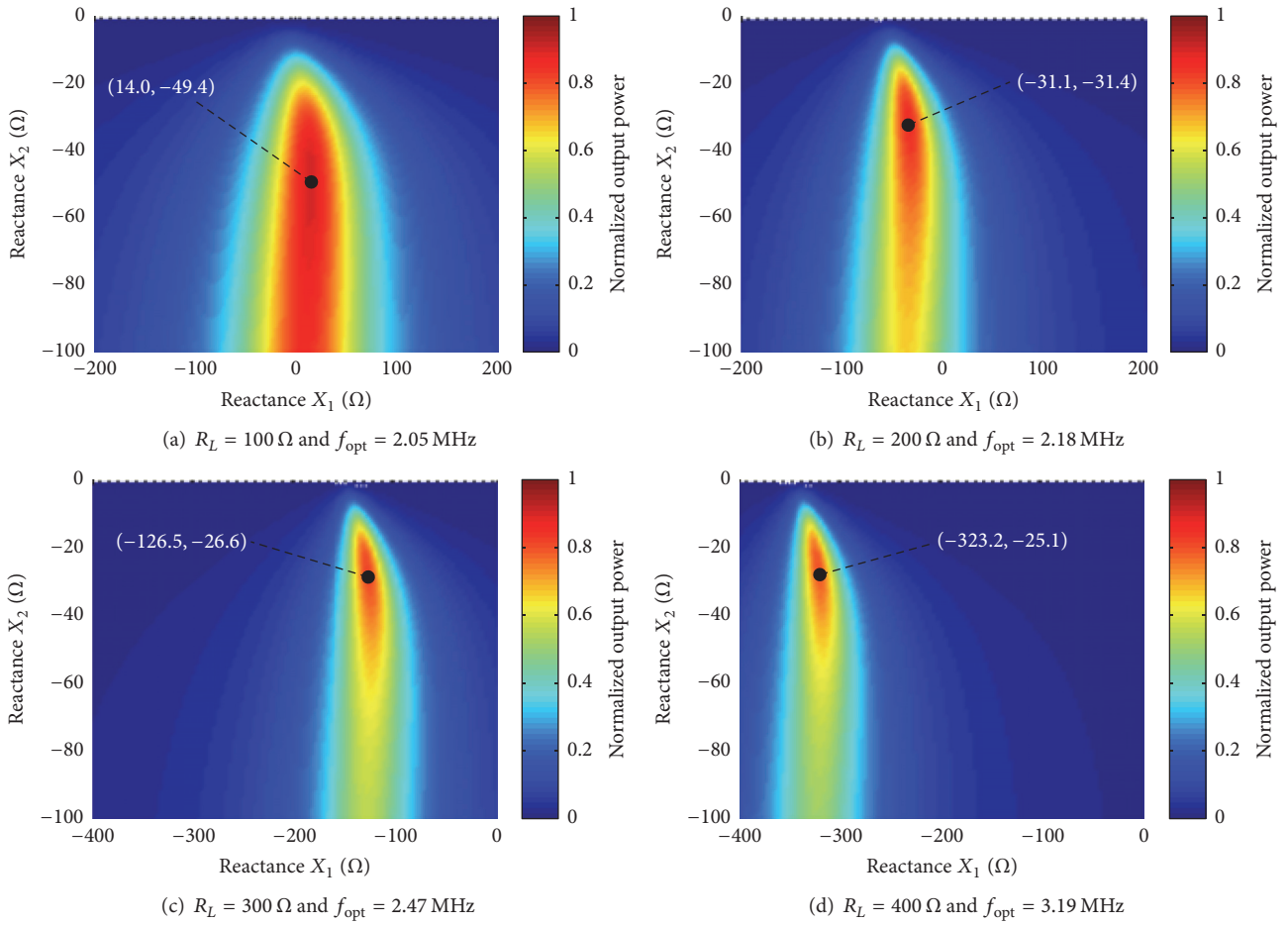

(a) $R_L = 100\,\Omega$ and $f_{\text{opt}} = 2.05$ MHz

(b) $R_L = 200\,\Omega$ and $f_{\text{opt}} = 2.18$ MHz

(c) $R_L = 300\,\Omega$ and $f_{\text{opt}} = 2.47$ MHz

(d) $R_L = 400\,\Omega$ and $f_{\text{opt}} = 3.19$ MHz

Figure 6: Calculated P_L versus X_1 and X_2. The load reactance $X_L = 0\,\Omega$.

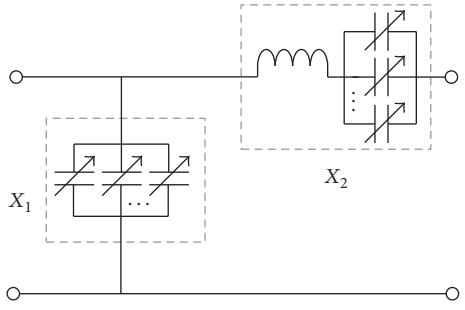

Figure 7: L-section IM network.

Table 2: Measured parameters of the experimental WPT system.

Parameters	Values
Tx coil inductance L_T	13.6 μH
Tx capacitor C_T	203.9 pF
Tx coil frequency f_T	3.0 MHz
Rx coil inductance L_R	10.6 μH
Rx capacitor C_R	260.5 pF
Rx coil frequency f_R	3.0 MHz
Source resistance R_S	50 Ω
Load resistance R_L	50, 100, 150, 200, 250 Ω
Load reactance X_L	−400, −200, 0, 200, 400 Ω

4.2. Experimental Results. In this section, the performances of three kinds of WPT systems are analyzed and compared, including the following:

System 1: The Original WPT System, As Shown in Figure 1. In order to achieve resonance, the source operating frequency is fixed at 3 MHz. The output power and power transmission efficiency of the system can be calculated using Equation (6) and Equation (8).

System 2: The Dual-Side Impedance-Matching WPT System, As Shown in Figure 2. The operating frequency is fixed at 3 MHz. Based on the method proposed in [18], the system can be adjusted to satisfy dual-side conjugate matching equations "$Z_{\text{in}} = Z_S^*$ and $Z_{\text{out}} = Z_L^*$" using two IM networks. The output power and power transmission efficiency of the system can be calculated by introducing "$Z_{\text{in}} = Z_S^*$ and $Z_{\text{out}} = Z_L^*$" into (6) and (8).

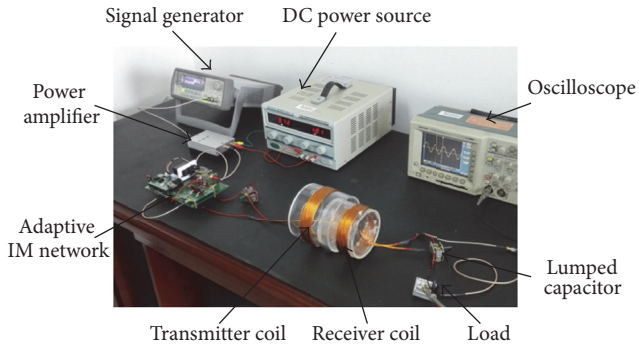

Figure 8: Experimental frequency-tracking and impedance-matching combined WPT system.

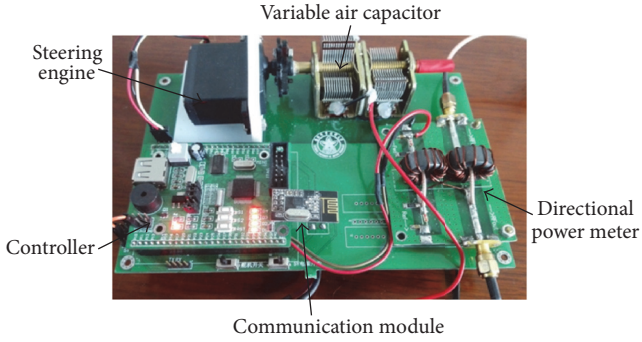

Figure 9: Adaptive impedance-matching circuit.

Table 3: Optimal frequencies and values of the compensating components. (The load resistance R_L is fixed at 50 Ω.)

X_L (Ω)	f_{opt} (MHz)	$X_{opt,1}$ (Ω)	$X_{opt,2}$ (Ω)
−400	5.3	−126.4	191.5
−200	4.3	−92.8	145.2
0	3.1	−126.0	11.1
200	2.2	−44.8	197.3
400	1.8	−33.1	307.5

System 3: The Proposed Frequency-Tracking and Impedance-Matching Combined WPT System, As Shown in Figure 3. The optimal frequencies used and the values of the compensating components in the proposed system are listed in Tables 3 and 4.

The measured power transmission efficiencies and output powers are listed in Tables 5 and 6. To simplify the analysis, the measured output powers are normalized to eliminate the influence of dimension. The normalized output power P_n is defined as $P_n = P_{out}/P_m$, where P_m is the maximum output power of the amplifier. In the experimental system, $P_m \approx 1.5$ W when the load is matched to 50 Ω.

As shown in Figures 10 and 11, the blue solid line represents the measured results of the original WPT system, the purple dashed line represents the calculated results of the original WPT system, the black dashed line represents the calculated results of the dual-side impedance-matching WPT system, the red solid line represents the measured results of the frequency-tracking and impedance-matching combined WPT system, and the green dashed line represents the calculated results of the frequency-tracking and impedance-matching combined WPT system.

Table 4: Optimal frequencies and values of the compensating components. (The load reactance X_L is fixed at 0 Ω.)

R_L (Ω)	f_{opt} (MHz)	$X_{opt,1}$ (Ω)	$X_{opt,2}$ (Ω)
50	3.1	−126.0	11.1
100	3.3	−49.5	0.1
150	3.6	−39.2	−59.2
200	4.3	−35.7	−152.5
250	6.5	−35.4	−393.5

Table 5: Measured power transmission efficiencies and output powers. (The load resistance R_L is fixed at 50 Ω.)

X_L (Ω)	P_{out} (W)		Efficiency (%)	
	S1	S3	S1	S3
−400	0.03	0.96	5.1	75.0
−200	0.26	1.15	25.0	81.8
0	1.21	1.27	85.4	83.6
200	0.26	1.08	22.3	73.9
400	0.02	0.83	3.3	59.1

Table 6: Measured power transmission efficiencies and output powers. (The load reactance X_L is fixed at 0 Ω.)

R_L (Ω)	P_{out} (W)		Efficiency (%)	
	S1	S3	S1	S3
50	1.20	1.28	84.2	85.3
100	1.06	1.23	77.8	82.0
150	0.90	1.23	70.6	80.4
200	0.75	1.20	66.7	78.2
250	0.69	1.16	64.3	77.5

Figure 10 shows that the power transmission efficiency and the output power of the original WPT system decrease dramatically when the load reactance deviates from $X_L = 0$ Ω. By employing the frequency-tracking and impedance-matching combined approach, the power transmission efficiency and the output power of the WPT system can be significantly improved.

In Figure 11, the similar trend can be found: the power transmission efficiency and the output power of the original WPT system decrease when the load resistance deviates from $R_L = 50$ Ω. Through the proposed approach, the WPT system can maintain high power transmission efficiency and output power even when the load resistance R_L changes. The experimental results suggest that the proposed frequency-tracking and impedance-matching combined system can significantly improve the robustness of the WPT system with load impedance variations.

From Figures 10 and 11, it can be observed that the measured power transmission efficiencies are lower than calculation results. It is because that the capacitors/inductances in the IM network are assumed to be ideal energy-storage

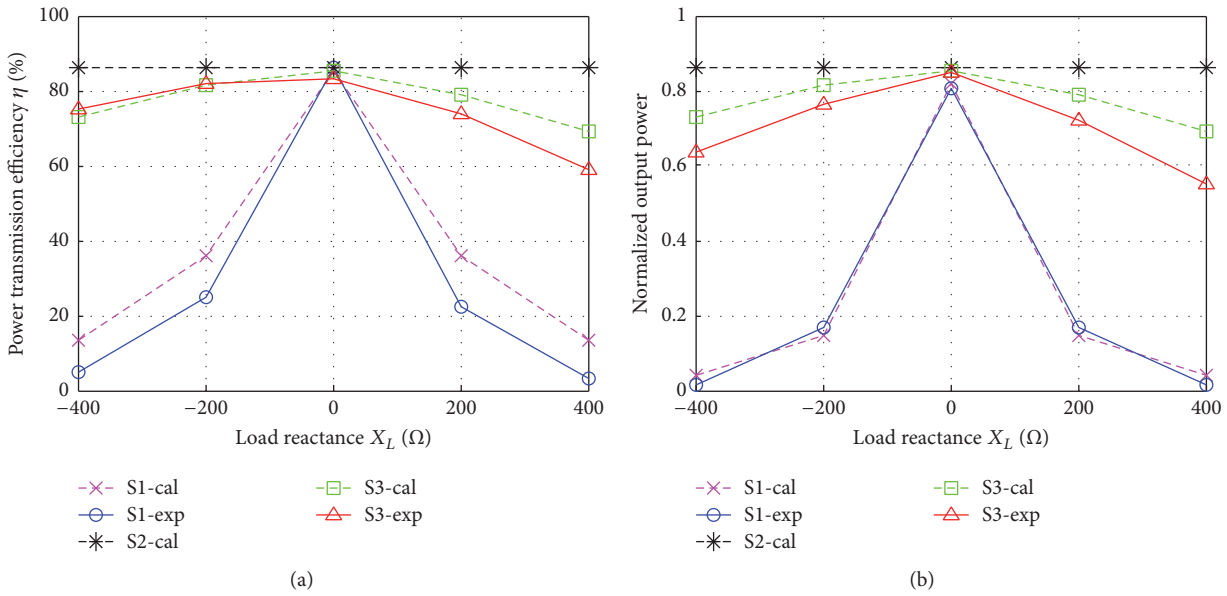

FIGURE 10: Comparison of three kinds of WPT systems. S1: the original WPT system; S2: the dual-side impedance-matching WPT system; S3: the frequency-tracking and impedance-matching combined WPT system. (a) Power transmission efficiency versus load reactance. (b) Output power versus load reactance.

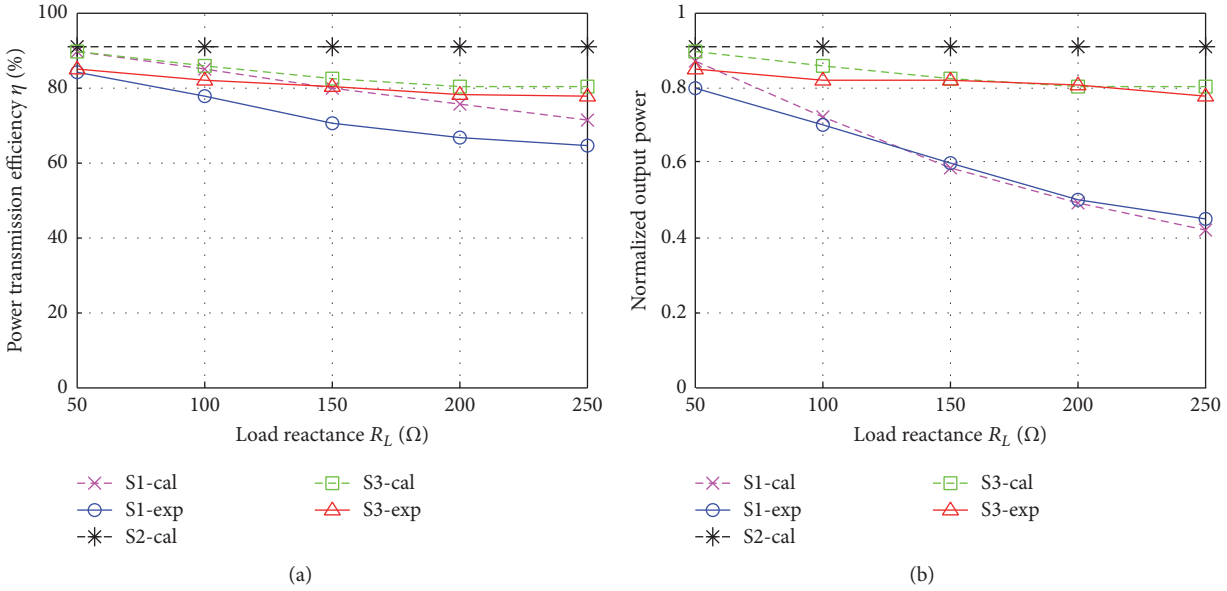

FIGURE 11: Comparison of three kinds of WPT systems. S1: the original WPT system; S2: the dual-side impedance-matching WPT system; S3: the frequency-tracking and impedance-matching combined WPT system. (a) Power transmission efficiency versus load resistance. (b) Output power versus load resistance.

components in calculations. But these components also consume part of the total energy in the form of heat and radiation in the practical WPT system. The more components are used, the more energy will be dissipated in the IM network. Therefore, adding too many impedance-matching components in the WPT circuit will decrease the total power transmission efficiency of the system.

As shown in Figures 10 and 11, the output powers of the proposed frequency-tracking and impedance-matching combined WPT system are lower than traditional dual-side impedance-matching WPT system. According to the maximum power transfer theorem [14, 30], the output power P_{out} will achieve the maximum value if the WPT system satisfies the dual-side conjugate matching equations "$Z_{\text{in}} = Z_S^*$ and $Z_{\text{out}} = Z_L^*$." However, using the proposed frequency-tracking and impedance-matching combined approach, only the transmitter-side can satisfy "$Z_{\text{in}} = Z_S^*$." Because no variable IM networks are used in the receiver circuit, "$Z_{\text{out}} = Z_L^*$"

are not satisfied. Therefore, the output power of the WPT system does not reach the maximum value in fact. Although the output power of the frequency-tracking and impedance-matching combined WPT system is lower than traditional dual-side impedance-matching WPT system, it can still maintain high values without adding more components in the receiver circuit.

In this study, the output power feedback at the receiver-side should be provided to the transmitter-side. There are two approaches to provide output power feedback to the transmitter-side. The mathematical approach requires only information of the input voltage U_1 and current I_1 at the transmitter-side, and then P_{out} can be calculated using (20), thereby eliminating the requirements of using wireless communication system.

$$U_2 = \frac{DU_1 - BI_1}{AD - BC},$$
$$I_2 = \frac{CU_1 - AI_1}{BC - AD}, \tag{20}$$
$$P_{\text{out}} = U_2 I_2.$$

However, in practice, the mathematical approach is very dependent on the accuracy of the measurements of U_1, I_1 and A, B, C, and D parameters, which are complex numbers. The wireless communication approach is more accurate and efficient but requires using wireless communication system to give feedback about P_{out} measurements to the transmitter-side. For the embedded applications, the size of the wireless communication unit can be further reduced so as to integrate it into the receiver.

Moreover, the selection of the operating frequency is important for resonant WPT systems. For many applications, the operating frequency of the WPT system is limited to a very narrow band (e.g., 6.765–6.795 MHz and 13.553–13.567 MHz according to the ISM band standard [15, 27]). In some previous studies [10–14], the feasibility and advantages of using frequency-tuning technique in a wider frequency range have also been demonstrated. Based on the frequency-tracking and impedance-matching combined approach proposed in this paper, the operating frequency of the WPT system should be adjusted in the range of a few megahertz to maximize the power transmission efficiency and output power, thereby eliminating the requirements of using receiver-side IM networks. The frequency range used in this study is commercially available and easy to implement in practical applications. Since fewer components are used in the receiver-side, the proposed approach is more suitable for some applications such as wireless power transfer for embedded devices.

5. Conclusions

To improve the robustness of wireless power transfer for embedded devices, a frequency-tracking and impedance-matching combined system is proposed in this paper. When the load impedance changes, the source operating frequency is optimized to increase the power transmission efficiency at first, and then the variable IM network in the transmitter circuit is automatically adjusted to increase the output power of the WPT system. An experimental system is implemented and measured, and a good agreement between the measurements and calculations is obtained. The results suggest that the proposed frequency-tracking and impedance-matching combined WPT system can quickly adapt to load impedance variations and maintain high power transmission efficiency and output power. Because no variable IM networks, relay coils, and other compensating components are used in the receiver circuit, the proposed approach is more beneficial to reduce the size, weight, and complexity of the receiver for embedded applications.

Competing Interests

The authors declare that they have no competing interests.

Acknowledgments

This work was supported by National Basic Research Program of China (2015CB057400).

References

[1] I. Mayordomo, T. Drager, J. A. Alayon, and J. Bernhard, "Wireless power transfer for sensors and systems embedded in fiber composites," in *Proceedings of the IEEE Wireless Power Transfer (WPT '13)*, pp. 107–110, Perugia, Italy, May 2013.

[2] A. Kumar, S. Mirabbasi, and M. Chiao, "Resonance-based wireless power delivery for implantable devices," in *Proceedings of the IEEE Biomedical Circuits and Systems Conference (BioCAS '09)*, pp. 25–28, IEEE, November 2009.

[3] B. J. Lee, A. Hillenius, and D. S. Ricketts, "Magnetic resonant wireless power delivery for distributed sensor and wireless systems," in *Proceedings of the IEEE Topical Conference on Wireless Sensors and Sensor Networks (WiSNet '12)*, pp. 13–16, Santa Clara, Calif, USA, January 2012.

[4] G. Monti, L. Corchia, E. De Benedetto, and L. Tarricone, "A wearable wireless energy link for thin-film batteries charging," *International Journal of Antennas and Propagation*, vol. 2016, Article ID 9365756, 9 pages, 2016.

[5] D. Ahn, S. Kim, J. Moon, and I.-K. Cho, "Wireless power transfer with automatic feedback control of load resistance transformation," *IEEE Transactions on Power Electronics*, vol. 31, no. 11, pp. 7876–7886, 2016.

[6] P. P. Mercier and A. P. Chandrakasan, "Rapid wireless capacitor charging using a multi-tapped inductively-coupled secondary coil," *IEEE Transactions on Circuits and Systems I: Regular Papers*, vol. 60, no. 9, pp. 2263–2272, 2013.

[7] M. Fu, T. Zhang, C. Ma, and X. Zhu, "Efficiency and optimal loads analysis for multiple-receiver wireless power transfer systems," *IEEE Transactions on Microwave Theory and Techniques*, vol. 63, no. 3, pp. 801–812, 2015.

[8] J. Kim, D.-H. Kim, and Y.-J. Park, "Analysis of capacitive impedance matching networks for simultaneous wireless power transfer to multiple devices," *IEEE Transactions on Industrial Electronics*, vol. 62, no. 5, pp. 2807–2813, 2015.

[9] M. Fu, T. Zhang, X. Zhu, P. C.-K. Luk, and C. Ma, "Compensation of cross coupling in multiple-receiver wireless power

transfer systems," *IEEE Transactions on Industrial Informatics*, vol. 12, no. 2, pp. 474–482, 2016.

[10] J. Park, Y. Tak, Y. Kim, Y. Kim, and S. Nam, "Investigation of adaptive matching methods for near-field wireless power transfer," *IEEE Transactions on Antennas and Propagation*, vol. 59, no. 5, pp. 1769–1773, 2011.

[11] N. Y. Kim, K. Y. Kim, J. Choi, and C.-W. Kim, "Adaptive frequency with power-level tracking system for efficient magnetic resonance wireless power transfer," *Electronics Letters*, vol. 48, no. 8, pp. 452–454, 2012.

[12] P. Si, A. P. Hu, S. Malpas, and D. Budgett, "A frequency control method for regulating wireless power to implantable devices," *IEEE Transactions on Biomedical Circuits and Systems*, vol. 2, no. 1, pp. 22–29, 2008.

[13] N. Y. Kim, K. Y. Kim, and C.-W. Kim, "Automated frequency tracking system for efficient mid-range magnetic resonance wireless power transfer," *Microwave and Optical Technology Letters*, vol. 54, no. 6, pp. 1423–1426, 2012.

[14] J. D. Heebl, E. M. Thomas, R. P. Penno, and A. Grbic, "Comprehensive analysis and measurement of frequency-tuned and impedance-tuned wireless non-radiative power-transfer systems," *IEEE Antennas and Propagation Magazine*, vol. 56, no. 4, pp. 44–60, 2014.

[15] T. C. Beh, M. Kato, T. Imura, S. Oh, and Y. Hori, "Automated impedance matching system for robust wireless power transfer via magnetic resonance coupling," *IEEE Transactions on Industrial Electronics*, vol. 60, no. 9, pp. 3689–3698, 2013.

[16] T. P. Duong and J.-W. Lee, "A dynamically adaptable impedance-matching system for midrange wireless power transfer with misalignment," *Energies*, vol. 8, no. 8, pp. 7593–7617, 2015.

[17] Y. Lim, H. Tang, S. Lim, and J. Park, "An adaptive impedance-matching network based on a novel capacitor matrix for wireless power transfer," *IEEE Transactions on Power Electronics*, vol. 29, no. 8, pp. 4403–4413, 2014.

[18] Y. Luo, Y. Yang, and Z. Chen, "Self-tuning wireless power transmission scheme based on on-line scattering parameters measurement and two-side power matching," *Scientific Reports*, vol. 4, article 4332, 2014.

[19] B.-H. Choi and J.-H. Lee, "Design of asymmetrical relay resonators for maximum efficiency of wireless power transfer," *International Journal of Antennas and Propagation*, vol. 2016, Article ID 8247476, 8 pages, 2016.

[20] M. Koizumi, K. Komurasaki, Y. Mizuno, and Y. Arakawa, "Wireless power feeding with strongly coupled magnetic resonance for a flying object," *Wireless Engineering and Technology*, vol. 3, no. 2, pp. 86–89, 2012.

[21] J. Kim and J. Jeong, "Range-adaptive wireless power transfer using multiloop and tunable matching techniques," *IEEE Transactions on Industrial Electronics*, vol. 62, no. 10, pp. 6233–6241, 2015.

[22] T. P. Duong and J.-W. Lee, "Experimental results of high-efficiency resonant coupling wireless power transfer using a variable coupling method," *IEEE Microwave and Wireless Components Letters*, vol. 21, no. 8, pp. 442–444, 2011.

[23] B. C. Park and J. H. Lee, "Adaptive impedance matching of wireless power transmission using multi-loop feed with single operating frequency," *IEEE Transactions on Antennas and Propagation*, vol. 62, no. 5, pp. 2851–2856, 2014.

[24] C. Florian, F. Mastri, R. P. Paganelli, D. Masotti, and A. Costanzo, "Theoretical and numerical design of a wireless power transmission link with GaN-based transmitter and adaptive receiver," *IEEE Transactions on Microwave Theory and Techniques*, vol. 62, no. 4, pp. 931–946, 2014.

[25] W. X. Zhong and S. Y. R. Hui, "Maximum energy efficiency tracking for wireless power transfer systems," *IEEE Transactions on Power Electronics*, vol. 30, no. 7, pp. 4025–4034, 2015.

[26] T. Diekhans and R. W. De Doncker, "A dual-side controlled inductive power transfer system optimized for large coupling factor variations and partial load," *IEEE Transactions on Power Electronics*, vol. 30, no. 11, pp. 6320–6328, 2015.

[27] Y. Yi, U. Buttner, Y. Fan, and I. G. Foulds, "Design and optimization of a 3-coil resonance-based wireless power transfer system for biomedical implants," *International Journal of Circuit Theory and Applications*, vol. 43, no. 10, pp. 1379–1390, 2015.

[28] D.-W. Seo, J.-H. Lee, and H. Lee, "Integration of resonant coil for wireless power transfer and implantable antenna for signal transfer," *International Journal of Antennas and Propagation*, vol. 2016, Article ID 7101207, 7 pages, 2016.

[29] R. Wu, S. Raju, M. Chan, J. K. O. Sin, and C. P. Yue, "Silicon-embedded receiving coil for high-efficiency wireless power transfer to implantable biomedical ics," *IEEE Electron Device Letters*, vol. 34, no. 1, pp. 9–11, 2013.

[30] D.-W. Seo, J.-H. Lee, and H.-S. Lee, "Optimal coupling to achieve maximum output power in a WPT system," *IEEE Transactions on Power Electronics*, vol. 31, no. 6, pp. 3994–3998, 2016.

[31] S. Cheon, Y.-H. Kim, S.-Y. Kang, M. L. Lee, J.-M. Lee, and T. Zyung, "Circuit-model-based analysis of a wireless energy-transfer system via coupled magnetic resonances," *IEEE Transactions on Industrial Electronics*, vol. 58, no. 7, pp. 2906–2914, 2011.

[32] T. Imura and Y. Hori, "Maximizing air gap and efficiency of magnetic resonant coupling for wireless power transfer using equivalent circuit and Neumann formula," *IEEE Transactions on Industrial Electronics*, vol. 58, no. 10, pp. 4746–4752, 2011.

[33] T. C. Beh, T. Imura, M. Kato, and Y. Hori, "Basic study of improving efficiency of wireless power transfer via magnetic resonance coupling based on impedance matching," in *Proceedings of the IEEE International Symposium on Industrial Electronics (ISIE '10)*, Bari, Italy, July 2010.

[34] X. Li, H. Zhang, F. Peng et al., "A wireless magnetic resonance energy transfer system for micro implantable medical sensors," *Sensors*, vol. 12, no. 8, pp. 10292–10308, 2012.

[35] B. H. Choi, E. S. Lee, J. Huh, and C. T. Rim, "Lumped impedance transformers for compact and robust coupled magnetic resonance systems," *IEEE Transactions on Power Electronics*, vol. 30, no. 11, pp. 6046–6056, 2015.

[36] S. Y. R. Hui, W. Zhong, and C. K. Lee, "A critical review of recent progress in mid-range wireless power transfer," *IEEE Transactions on Power Electronics*, vol. 29, no. 9, pp. 4500–4511, 2014.

[37] M. Zargham and P. G. Gulak, "Maximum achievable efficiency in near-field coupled power-transfer systems," *IEEE Transactions on Biomedical Circuits and Systems*, vol. 6, no. 3, pp. 228–245, 2012.

[38] L. Chen, S. Liu, Y. C. Zhou, and T. J. Cui, "An optimizable circuit structure for high-efficiency wireless power transfer," *IEEE Transactions on Industrial Electronics*, vol. 60, no. 1, pp. 339–349, 2013.

[39] H. M. Nemati, C. Fager, U. Gustavsson, R. Jos, and H. Zirath, "Design of varactor-based tunable matching networks for dynamic load modulation of high power amplifiers," *IEEE*

Transactions on Microwave Theory and Techniques, vol. 57, no. 5, pp. 1110–1118, 2009.

[40] E. M. Fall, F. Domingue, S. Fouladi, and R. R. Mansour, "A novel reconfigurable impedance matching network using tunable MEMS capacitive and inductive components," in *Proceedings of the 41st European Microwave (EuMC '11)*, pp. 1225–1228, October 2011.